J Incl Phenom Macrocycl Chem
DOI 10.1007/s10847-013-0348-4

ORIGINAL ARTICLE

Investigating the inclusion of the Ag(I)-nimesulide complex into β-cyclodextrin: studies in solution and in the solid state

Raphael E. F. de Paiva · Camilla Abbehausen · Fernando R. G. Bergamini · Andre L. Thompson · Danilo A. Alves · Marcelo Lancellotti · Pedro P. Corbi

Received: 14 May 2013 / Accepted: 15 June 2013

Abstract The present work describes the preparation and characterization of inclusion systems involving β-CD and the silver(I) nimesulide coordination complex (Ag-NMS), prepared by kneading (*K*) and co-evaporation (*CE*) methods. Solid state characterization by DSC, XRD and IR vibrational spectroscopic measurements provided remarkable evidences of the formation of true inclusion systems. Solution measurements provided information about the inclusion mode. The UV–Vis spectroscopy was used to obtain the association constants by the Scatchard method, and the value obtained was 370 ± 2 L mol^{-1}. The ^{1}H NMR spectroscopic measurements indicate a total inclusion of the guest into the cavity. A 2D NOESY experiment was carried out for the inclusion complex. The spectrum shows that hydrogens 3–6 of the cyclodextrin clearly correlate with the protons of the phenoxy ring of nimesulide in the Ag-NMS coordination compound, which confirms the formation of the inclusion complex. The antibacterial activities of the Ag-NMS and *CE*-[(Ag-NMS)·β-CD] inclusion system were evaluated by the well diffusion method over *Escherichia coli* and *Pseudomonas aeruginosa* (Gram-negative) and *Staphylococcus aureus* (Gram-positive) pathogenic bacterial strains. The observed data shows the significant antibacterial activity of the Ag-NMS coordination complex, and no activity for the inclusion complex under the same considered conditions.

Keywords Silver(I) · Nimesulide · β-Cyclodextrin · Inclusion chemistry · NOESY NMR

Abbreviations

NMS	Nimesulide
Ag-NMS	Silver(I) coordination complex with nimesulide
CD	Cyclodextrin
DSC	Differential scanning calorimetry
XRD	X-ray diffractometry
IR	Infrared
NMR	Nuclear magnetic resonance
NOESY	Nuclear overhauser effect spectroscopy NMR spectroscopy
UV–Vis	Ultraviolet–Visible spectroscopy
TMS	Tetramethylsilane
DMSO	Dimethyl sulfoxide
DMF	Dimethylformamide
HG	Host–guest inclusion complex
ε	Molar extinction coefficient
ε_H	Molar extinction coefficient of the host molecule
ε_G	Molar extinction coefficient of the guest molecule
ε_{HG}	Molar extinction coefficient of the host–guest inclusion complex
ATCC	American type collection cell
MH	Mueller-Hinton agar
BHI	Brain-heart infusion medium
CFU	Colony forming unit
MIC	Minimum inhibitory concentration

Electronic supplementary material The online version of this article (doi:10.1007/s10847-013-0348-4) contains supplementary material, which is available to authorized users.

R. E. F. de Paiva · C. Abbehausen · F. R. G. Bergamini · A. L. Thompson · P. P. Corbi (✉)
Inorganic Chemistry Department, Institute of Chemistry, University of Campinas—UNICAMP, P.O. Box 6154, Campinas, SP 13083-970, Brazil
e-mail: ppcorbi@iqm.unicamp.br

R. E. F. de Paiva
e-mail: raphael.enoque@gmail.com

D. A. Alves · M. Lancellotti
Laboratory of Biotechnology, Institute of Biology, University of Campinas, UNICAMP, Campinas, SP 13083-970, Brazil

Published online: 23 June 2013

Introduction

Silver complexes have been extensively studied as antibacterial agents since the discovery of the antibacterial activities of silver(I) sulphadiazine (Ag-SD) in 1960s [1, 2]. The Ag-SD compound has a broad spectrum of activity against pathogenic bacterial strains, and it has been used in the treatment of severe burns. This aspect has stimulated the search of new and more effective silver(I) compounds for the treatment of multi-resistant bacterial strains as an alternative to commercial antibiotics [3–5].

Although effective against different bacterial strains, one of the major problems of silver complexes, mainly when biological systems are taken into account, are their poor solubility in water and in other common solvents [6]. Since silver(I) ion has a closed-shell electronic configuration, the insolubility of such compounds may be related to the Ag(I) center capability to adopt diverse coordination numbers with no strong energetic preference for any particular geometry [7]. This capability may generate extended solid structures, leading to polymeric and less soluble compounds. In this context, several reports have been made in which silver(I) complexes are described as extended 1D, 2D and 3D polymeric structures [8–13].

One of the possible approaches to increase the solubility of such silver coordination compounds is their inclusion into the cavity of cyclodextrins (CD) [14–17]. CD are cyclic torus-like oligosaccharides consisting of several glucopyranose rings α-1,4-linked through glucosidic bonds [15, 16]. The most common CD contains six, seven and eight glucopyranose units, being called as α-, β- and γ-cyclodextrins, respectively. These macromolecules present a hydrophobic cavity and a hydrophilic surface, being able to form host–guest (HG) complexes by the inclusion of apolar moieties of different compounds into the CD cavity. The hydrophilic surface of CD turns the guest more soluble in polar solvents [15, 16].

The inclusion phenomena is limited by the molecular size, and it is driven by the type of interaction involved [18]. The HG interaction is mostly due to van der Waals forces and, especially for β-CD, the compounds that possesses benzylic rings or an adamantyl moiety were shown to be more suitably included since they are able to overcome the geometric restriction [19, 20].

Several coordination compounds with different classes of organic ligands can also be considered for inclusion into CDs. In this context, the inclusion of metallocene and metallocene-derived coordination compounds of metals such as Fe, Mo, Eu, Nb and Ti into the cavity of CDs have been extensively studied [21–32].

The inclusion of other non-organometallic complexes has also been reported. A vanadium compound with a hydrazone, derived from the condensation of salicylaldehyde and the biphenyl-4-carboxilic acid (salhybiph), K[VO_2(salhybiph)], was included into the cavity of α-CD and β-CD forming 1:1 and 1:2 (guest/host) complexes, respectively [33]. Braga et al. reported the interaction studies of β-CD and permethylated β-CD with a chloride 2,2′-bipyridine trithiacyclononane ruthenium(II) coordination compound [34]. This complex was designed to be used as a DNA intercalator in order to act as an antitumoral agent.

Other systems dealing with coordination compounds bonded to modified cyclodextrin moieties were also reported in the literature. Legrand et al. [35] recently reported the synthesis of a new silver(I) organometallic compound based on a β-cyclodextrin-imidazolium salt, which has been considered as a catalyst in the Suzuki cross-coupling reaction. The silver(I) coordination compounds presented the coordination through to the C-1 carbon of the imidazolium moiety of the β-cyclodextrin salt.

Nimesulide (NMS, Fig. 1a) is a non-steroidal anti-inflammatory sulfonamide which exhibits benzyl and nitro substituted rings. It has been used in the treatment of acute or chronic inflammatory processes of the respiratory tract and the oral cavity, tendinitis, rheumatoid arthritis and dysmenorrhea [36].

Recently, a silver complex with nimesulide (Ag-NMS, Fig. 1b) was synthesized and characterized [37]. Nimesulide coordinates to Ag(I) through the nitrogen and oxygen atoms of the sulphonamide group. This compound is poorly soluble in water, but is soluble in dimethyl sulfoxide (DMSO), dimethylformamide (DMF), ethanol and methanol. The poor solubility not only limits other medical applications, but also limits the ability to study the mechanism of action of the Ag-NMS in biological medium.

The inclusion of nimesulide into β-CD was previously reported, with an increase of its solubility in water [38]. The nimesulide molecule is prone to be included into the cavity, due to its structure with two aromatic rings.

This work deals with the inclusion of the Ag-NMS coordination compound into the cavity of β-CD and its characterization in the solid state by differential scanning calorimetry (DSC), X-ray diffractometry (XRD) and infrared (IR) spectroscopic measurements and also in solution by nuclear magnetic resonance (^{1}H NMR, NOESY) and ultraviolet–visible (UV–Vis) spectroscopies.

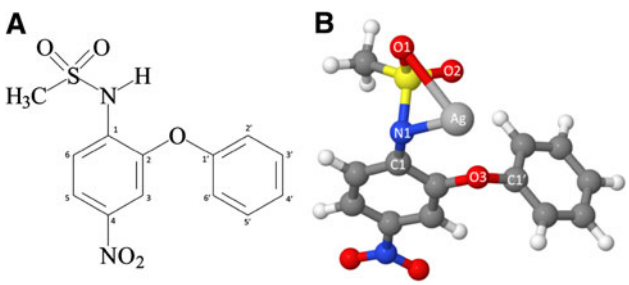

Fig. 1 Structures of **a** NMS and **b** Ag-NMS [37]

Antibacterial studies were also performed in order to evaluate the effect of the inclusion over the antibacterial activity of the Ag-NMS complex.

Experimental section

Reagents and equipments

Nimesulide (>99 %) and analytical grade silver(I) nitrate ($AgNO_3$) were purchased from Sigma-Aldrich laboratories. Potassium hydroxide (>85 %) and β-cyclodextrin (>99 %) were purchased from Fluka. The IR spectra of the compounds were measured from 4,000 to 400 cm^{-1} using an ABB Bomen MB Series FT-IR spectrophotometer; samples were prepared as KBr pellets. DSC analyses were performed on a TA Instruments 2910 in the range 25–225 °C (oxidant atmosphere, 10 °C min^{-1} heating rate). X-ray diffraction data of the polycrystalline samples were acquired on a Shimadzu X-ray spectrometer XRD6000, with a Cu Kα radiation (λ = 1.54060 Å).

The UV–Vis spectra of the inclusion systems were recorded on a Hewlett-Packard 8453A diode array spectrophotometer in the range 100–1,100 nm using 10.00 mm quartz cuvettes. The ^1H nuclear magnetic resonance (^1H-NMR) spectra of β-CD, Ag-NMS, co-evaporated NMS inclusion system (*CE*-[(NMS)·β-CD]) and co-evaporated Ag-NMS inclusion system (*CE*-[(Ag-NMS)·β-CD]) were recorded on a Bruker Avance III spectrometer (400 MHz, 9.395 T), using a 5-mm probe at 25 °C applying a 90° excitation pulse with duration of 8.40 μs, spectral width of 3.3 kHz, acquisition time of 4.56 s and relaxation delay of 1 s. The 2D nuclear overhauser effect spectroscopic data (NOESY) were acquired for the samples *CE*-[(NMS)·β-CD] and *CE*-[(Ag-NMS)·β-CD] in the same equipment applying a 90° pulse of 8.40 μs and a 180° pulse of 16.80 μs with a mixing time of 800 ms and relaxation delay of 1 s. Samples were prepared in D_2O (99.9 % deuterium content). All samples were prepared in concentrations of 10 mg mL^{-1}, except for Ag-NMS, which was prepared with a maximum concentration of 2 mg mL^{-1}.

Synthesis of the Ag-NMS compound

The Ag-NMS coordination compound was synthesized as previously reported in the literature [37]. Anal. Calc. for $AgC_{13}H_{11}N_2O_5S$ (%): C, 37.6; H, 2.7; N, 6.7. Found (%): C, 37.8; H, 2.4; N, 6.7. The yield of the synthesis was 85 %.

Preparation of the solid inclusion systems

The solid inclusion systems were prepared as previously reported in the literature for NMS [38]. The experimental procedures are described below.

Kneaded systems

The kneaded systems with β-CD for both NMS and Ag-NMS were prepared using 1:1 and 1:2 molar ratios of compound/β-CD. The mixtures were grinded in a mortar with 10.0 mL of a water/ethanol (1:1 v/v) solution. The pastes were kneaded for 45 min and then dried at 45 °C. The dried mass was finally powdered.

Co-evaporated systems

The co-evaporated systems with β-CD for both NMS and Ag-NMS were prepared by the addition of $6.0 \cdot 10^{-5}$ mol of β-CD and $6.0 \cdot 10^{-5}$ mol of NMS or Ag-NMS in 10.0 mL of a water/ethanol (1:1 v/v) solution. The resulting mixtures were stirred for 48 h and evaporated at 45 °C until dryness. The dried masses were then powdered.

Determination of the association constants in solution

Both [(NMS)·β-CD] and [(Ag-NMS)·β-CD] inclusion complexes were prepared using a fixed amount of NMS or Ag-NMS and increasing amounts of β-CD as presented in the Table 1. The samples were prepared suspending β-CD and NMS or Ag-NMS in 10.0 mL of water on a series of 25 mL stoppered Erlenmeyer flasks, and then the mixtures were shaken in a shaker water bath, at the fixed temperature of 25.0 ± 0.1 °C. After 48 h of shaking, aliquots of 2.0 mL were filtered and the absorbances were measured at 397 nm. Samples were also taken after 60 and 72 h in order to evaluate the extension of the inclusion. Solutions containing solely the same corresponding amounts of β-CD were used as blank for the UV–Vis measurements.

Antibacterial assays

Five pathogenic bacterial strains, *Escherichia coli* ATCC 25922, *Pseudomonas aeruginosa* ATCC 27853, *Staphylococcus aureus* ATCC 25923, *S. aureus* BEC9393 and

Table 1 Experimental conditions for the determination of the inclusions constants of NMS and Ag-NMS in β-CD

Solution	Guest molecule	β-CD
N1	NMS $2.7\ 10^{-5}$ mol (0.0083 g)	–
N2		$7.5\ 10^{-6}$ mol (0.0093 g)
N3		$3.5\ 10^{-5}$ mol (0.0405 g)
N4		$6.4\ 10^{-5}$ mol (0.0723 g)
N5		$9.1\ 10^{-5}$ mol (0.1036 g)
C1	Ag-NMS $2.7\ 10^{-5}$ mol (0.0112 g)	–
C2		$7.5\ 10^{-6}$ mol (0.0093 g)
C3		$3.5\ 10^{-5}$ mol (0.0405 g)
C4		$6.4\ 10^{-5}$ mol (0.0723 g)

S. aureus Rib1 were selected. Stock solutions of *CE*-[(NMS)·β-CD] and *CE*-[(Ag-NMS)·β-CD] were prepared in water (10.0 mg mL^{-1}), while Ag-NMS was previously dissolved in 500 µL of EtOH 70 % and than diluted with 4.5 mL of water, giving a final solution with the concentration of 10.0 mg mL^{-1}. Sufficient inocula of the bacterial strains were added to a 96 multiwell plate until the turbidity equaled 0.5 McFarland ($\sim 1.5 \times 10^8$ CFU mL^{-1}). The tested compounds were sequencially diluted into the multiwell plate. The negative control was obtained by leaving one of the wells of each bacterial strain with no addition of the considered compounds, while vancomycin and chloramphenicol were used as positive controls against the Gram-negative and Gram-positive bacterial strains, respectively. The minimal inhibitory concentrations (MIC) were estimated following the recommendations of the Clinical and Laboratory Standards Institute (CLSI) [39] and performed in triplicate.

Results and discussion

Evaluation of the inclusion in the solid-state

As described, the [(Ag-NMS)·β-CD] solid inclusion systems were obtained by two different preparation methods, kneading and co-evaporation. These strategies were previously reported in the preparation of NMS inclusion systems by Nalluri et al. [38], where kneaded systems in a 1:2 guest:host molar ratio generated a solid with high water solubility. The [(Ag-NMS)·β-CD] inclusion complexes prepared by both methods presented aqueous solubility in a concentration of 10 mg mL^{-1}, which is desirable for pharmaceutical formulations. In addition, the solubility improvement is an evidence of formation of an inclusion complex.

Differential scanning calorimetry

Nimesulide, Ag-NMS and their inclusion complexes in β-CD prepared by kneaded and co-evaporated method were studied by DSC. The DSC curves are presented in Fig. 2.

The DSC curve for NMS presents an endothermic peak at 151.0 °C which corresponds to the melting point, Fig. 2b [38], No endothermic peaks are observed for Ag-NMS in the temperature range 25–200 °C, Fig. 2c. The β-CD curve shows a broad endothermic peak which may be related to the dehydration process followed by its melting point, centered at 183.3 °C, Fig. 2a.

The NMS inclusion systems prepared by kneading process, *K*-[(NMS)·β-CD], (see Fig. 2d, e) shows a sharp endothermic peak at 145 °C, which is shifted by 6 °C from the NMS. The observed result indicates a partial inclusion

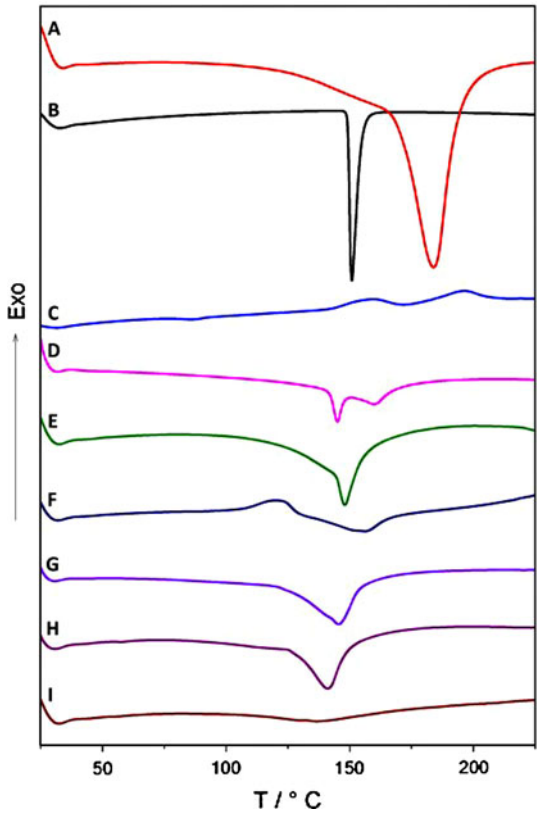

Fig. 2 DSC curves of (*A*) β-CD, (*B*) NMS, (*C*) Ag-NMS, (*D*) *K*-[(NMS)·β-CD] 1:1 system, (*E*) *K*-[(NMS)·β-CD] 1:2 system, (*F*) *K*-[(Ag-NMS)·β-CD] 1:1 system, (*G*) *K*-[(Ag-NMS)·β-CD] 1:2 system, (*H*) *CE*-[(NMS)·β-CD] system and (*I*) *CE*-[(Ag-NMS)·β-CD] system

of NMS in β-CD. In this case, the system was prepared in two different molar ratios. The 1:2 molar composition (Fig. 2e) showed better results. However, it still shows two different peaks, a sharp and a broad one. For the co-evaporated system, *CE*-[(NMS)·β-CD] (Fig. 2h), a single broad peak centered at 141 °C is observed, indicating a complete inclusion of NMS. These results are in agreement with those previously reported [38].

For the Ag-NMS inclusion complexes, the kneading procedure (*K*-[(Ag-NMS)·β-CD]) was also used to prepare systems with two different molar ratios, 1:1 and 1:2 Ag-NMS/β-CD, and their DSC curves can be seen in Fig. 2f, g, respectively. The shift and broadening of β-CD peak indicate the formation of inclusion complexes. The 1:2 guest/host molar ratio seems to be a better system, due to the presence of a sharper melting peak. The co-evaporated system, in this case, shows no peaks and could not be evaluated properly (Fig. 2i). Nevertheless, it is important to emphasize that the absence of a characteristic fusion peak does not indicate that *CE* method is inadequate for preparation of the [Ag-NMS·β-CD] system. Since the Ag-NMS itself does not present any characteristic fusion peak, the absence of this thermal phenomena in the inclusion system

is not sufficient to conclude that the inclusion did not occurred. In order to fully evaluate the formation and the extension of the inclusion, additional measurements by other techniques were considered.

X-ray powder diffraction

The diffraction patterns of the inclusion complexes are expected to be distinct from the patterns obtained by the simple superposition of each isolated component of the inclusion system. The X-ray diffractograms of kneaded systems, co-evaporated systems, β-CD, NMS and Ag-NMS are presented in the Fig. 3.

As reported by Sanphui et al. [40], nimesulide can crystallizes in at least two forms, referred as Form I and Form II. The XRD pattern and the relative intensities of the NMS used in this study (Fig. 3a) matches with Form I. The non-included Ag-NMS shows no defined diffraction peaks (Fig. 3c).

The X-ray diffractograms of the HG systems were compared to the free β-CD diffractogram (Fig. 3b). The most pronounced change observed upon inclusion for all formulations is the disappearance of the diffraction peak of β-CD at $2\theta = 4.66°$. Also, an amorphization process for all formulations is observed, which is indicative of the inclusion complexes formation.

The diffractograms of NMS inclusion complexes prepared by kneading (Fig. 3d, e) show some degree of crystallinity, with the diffraction peaks being compatible with β-CD and with free NMS. However, the most intense β-CD diffraction at $2\theta = 4.66°$ and the NMS intense diffraction appears at $2\theta = 5°$ are observed with very low relative intensities. Both 1:1 and 1:2 molar ratios present very similar diffraction patterns. The diffractogram of NMS inclusion complex prepared by co-evaporation (Fig. 3h) also presents some degree of crystallinity with a similar pattern when compared to those obtained by the kneaded method. The amorphization points to the formation of inclusion complexes. This result is in agreement with the DSC evaluation.

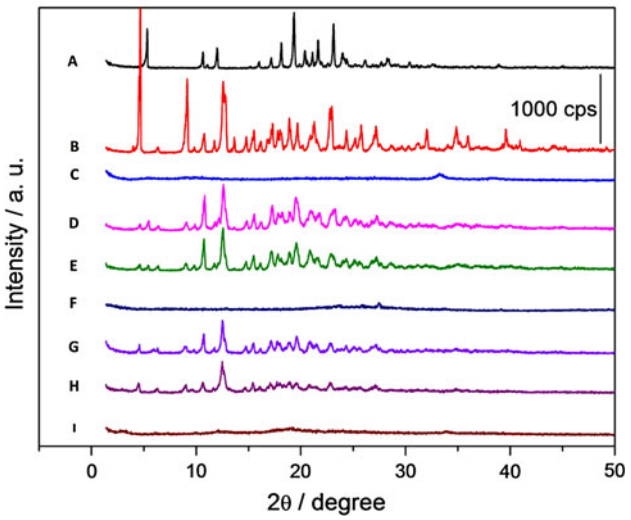

Fig. 3 XRD profiles of (*A*) β-CD, (*B*) NMS, (*C*) Ag-NMS, (*D*) *K*-[(NMS)·β-CD] 1:1 system, (*E*) *K*-[(NMS)·β-CD] 1:2 system, (*F*) *K*-[(Ag-NMS)·β-CD] 1:1 system, (*G*) *K*-[(Ag-NMS)·β-CD] 1:2 system, (*H*) *CE*-[(NMS)·β-CD] system and (*I*) *CE*-[(Ag-NMS)·β-CD] system

The diffractograms of the Ag-NMS inclusion systems prepared by kneading, on the other hand, presents different behaviors according to the molar ratio. The *K*-[(Ag-NMS)·β-CD] 1:1 formulation presents no crystallinity (Fig. 3f), while the *K*-[(Ag-NMS)·β-CD] 1:2 formulation presents the diffraction pattern similar to β-CD (Fig. 3g). The similarity between the XRD profiles of many of the formulations with the free β-CD can be due to the presence of the intermolecular forces between the host molecules, mainly hydrogen bonds, responsible for the maintenance of the typical packing structure of β-CD even in the inclusion complexes. The *CE*-[(Ag-NMS)·β-CD] systems show an amorphous pattern (Fig. 3i). This result shows that distinct inclusion complexes have been formed according to the chosen procedure.

Infrared spectroscopic measurements

The Fig. 4 shows the IR spectra of free β-CD, NMS, Ag-NMS and all the solid host/guest formulations.

The NMS inclusion complexes present vibrational modes of the polar groups almost unchanged. The sharp (N–H) stretching mode in the free NMS at 3,284 cm^{-1} (Fig. 4A) appears as a small shoulder at ~3,290 cm^{-1} in the kneaded inclusion complexes (Fig. 4d, e). The broad OH stretching mode due to aggregation of β-CD and water almost covers this absorption. Both ν_{as}(O=S=O) and ν_s(O=S=O) vibration modes appear in *K*-[(NMS)·β-CD] 1:1 (Fig. 4d) and *K*-[(NMS)·β-CD] 1:2 (Fig. 4e) in the same position of the free guest. The two intense characteristic bands of the nitro (NO_2) group, $\nu_{as}(NO_2)$ at 1,522 cm^{-1} and $\nu_s(NO_2)$ at 1,317 cm^{-1} in the free NMS, remain unchanged in the inclusion complexes. Regarding the β-CD, the δ(C–O–H) remains almost unchanged, along with both ν(C–O–C) asymmetrical and symmetrical stretching modes. The IR spectrum of *CE*-[(NMS)·β-CD] system (Fig. 4h), on the other hand, shows no significant changes with reference to the inclusion. Therefore, the IR data in this case is not conclusive concerning the formation of an inclusion system.

The IR spectra of the kneaded Ag-NMS inclusion systems (Fig. 4f, g) present particular changes. The ν_{as}(O=S=O) and ν_s(O=S=O) of the sulfonamide group in the free Ag-NMS (Fig. 4c) appears at 1,342 and 1,153 cm^{-1} respectively. Upon inclusion, these bands are shifted to 1,292 and 1,157 cm^{-1},

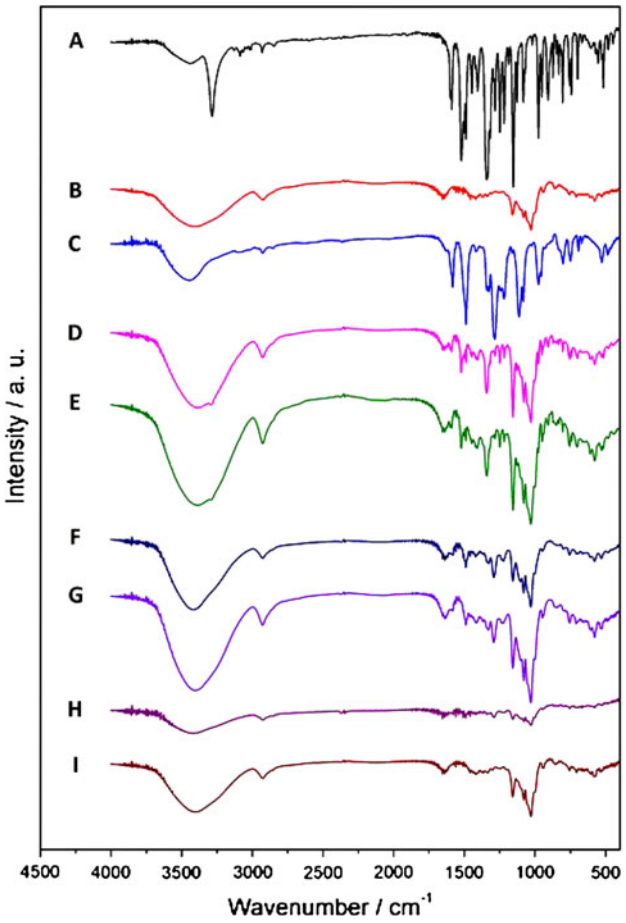

Fig. 4 IR vibrational spectra of (*A*) NMS, (*B*) β-CD, (*C*) Ag-NMS, (*D*) *K*-[(NMS)·β-CD] 1:1 system, (*E*) *K*-[(NMS)·β-CD] 1:2 system, (*F*) *K*-[(Ag-NMS)·β-CD] 1:1 system, (*G*) *K*-[(Ag-NMS)·β-CD] 1:2 system, (*H*) *CE*-[(NMS)·β-CD] system and (*I*) *CE*-[(Ag-NMS)·β-CD] system

respectively. This data suggests that the sulfonamide group of the Ag-NMS complex in the inclusion systems present an interaction with the hydroxyl groups of β-CD.

Studies in aqueous solution

UV–Vis Spectroscopic data

The UV–Vis spectra of NMS and Ag-NMS inclusion complexes were evaluated in order to determine their association constants. The UV–Vis spectra were acquired up to 72 h after the beginning of the experiment. No absorbance changes were observed for all samples after 48 h, which means that both [(NMS)·β-CD] and [(Ag-NMS)·β-CD] solution systems reaches the equilibrium in 48 h.

Both NMS and Ag-NMS UV–Vis spectra exhibit an electronic transition at 390 nm. This transition was previously investigated using TD-DFT, being assigned as a HOMO–LUMO π–π* transition [37]. Apart for small energy shifts, calculations confirm that the coordination of NMS to Ag(I) does not change the nature of the transitions.

Upon inclusion, the UV–Vis spectra show two phenomena. First, the π–π* transition is shifted to ∼397 nm. Since this transition is assigned to the HOMO–LUMO transition, the bathochromic shift suggests that the inclusion reduces the energy difference between the frontier orbitals for both NMS and Ag-NMS. Furthermore, the molar extinction coefficient (ε) of the HOMO–LUMO transition is enhanced upon the inclusion, which means that ε_{HG} is higher than both ε_H and ε_G.

Determination of the association constants in solution

In order to obtain the association constant (K_a) for both [(NMS)·β-CD] and [(Ag-NMS)·β-CD] systems in aqueous solution, the following equilibrium must be considered:

$$H + G \rightleftharpoons HG \tag{1}$$

where the host (H) is β-CD, the inclusion guest (G) is NMS or Ag-NMS and the inclusion complex (HG) is [(NMS)·β-CD] or [(Ag-NMS)·β-CD]. The UV–Vis absorbance of a system where all the three species H, G and HG are present is given by

$$A = \epsilon_H b[H] + \epsilon_G b[G] + \epsilon_{HG} b[HG] \tag{2}$$

The guest compound is in equilibrium with the inclusion complex HG, so the [HG] and [G] are constrained:

$$A = \epsilon_G b[G]_0 + \Delta\epsilon_{HG} b[HG] \tag{3}$$

where $\Delta\epsilon_{HG} = \epsilon_{HG} - \epsilon_H - \epsilon_G$ and $[G]_0$ is the starting concentration of the guest molecule. At last, combining (3) with the definition of K_a, a nonlinear expression is obtained, describing absorption changes for 1:1 inclusion systems

$$\frac{\Delta A}{b} = \frac{\Delta\epsilon_{HG} K_a [H][G]_0}{1 + K_a[H]} \tag{4}$$

One approach to linearize Eq. 4 is the Scatchard method [41]. Here, this method is used with a slight modification. The systems described by Scatchard, and most of the β-CD inclusion systems, present negative values of ΔA upon inclusion. Both NMS and Ag-NMS, on the other hand, presents positive values of ΔA. Accounting to this phenomenon, the linearization equation obtained is

$$\frac{\Delta A}{b[H]} = \frac{\Delta A K_a}{b} + \Delta\epsilon_{HG} K_a [G]_0 \tag{5}$$

Therefore, with this approach, it is possible to obtain K_a as the slope of the plotting of ΔA/b[H] against ΔA/b.

Figure 5 shows the UV–Vis spectra of the Ag-NMS solution systems presented in Table 1. The plots of ΔA/b[H] versus ΔA/b for both NMS and Ag-NMS are given in

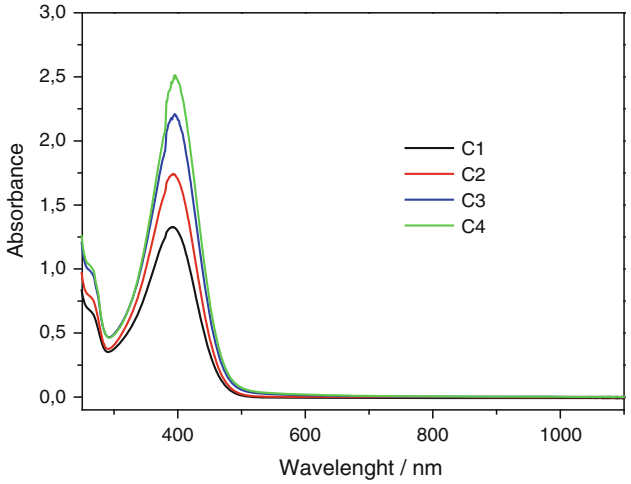

Fig. 5 UV–Vis spectra of Ag-NMS solutions systems used to determine K_a (concentrations described in Table 1)

Supporting Information. The calculated K_a values obtained from those plots for NMS and Ag-NMS were 367 ± 3 and 370 ± 2 L mol^{-1}, respectively. Both compounds are well described by a single linear regression, which indicates the existence of a single association constant for each system. For comparative purposes, the β-CD inclusion complex of nitrobenzene presents K_a = 154 L mol^{-1} (pH = 7.0) [42] and the β-CD inclusion complex of p-nitrophenol presents K_a = 130 L mol^{-1} for the neutral species [43].

^{1}H-NMR spectroscopic studies

The nuclear magnetic resonance spectroscopy provides structural information of supramolecular systems by direct observation. The difference in the proton chemical shifts between the free guest, the host species and the suggested inclusion complex provides information about the inclusion process. The protons of the host are shown in Fig. 6, while the ^{1}H NMR spectra of the free guest (Ag-NMS), free host (β-CD) and the *CE*-[(Ag-NMS)·β-CD] system can be observed in Figs. 7 and 8. The full ^{1}H NMR spectra are presented in Supporting Information.

The full spectrum of the inclusion complex confirms that no free β-CD is present. The structure in Fig. 6 demonstrates that the inner cavity hydrogens 3 and 5 are the most affected protons in the structure of the β-CD by the formation of inclusion complexes. It is possible to observe in Fig. 7 that hydrogen atoms 3 and 5 of β-CD are both shifted upfiled by the formation of the inclusion complex while no shifts are observed for the other protons of the β-CD, confirming the formation of an inclusion complex between Ag-NMS and β-CD. The external hydrogens 2 and 4 remain unchanged upon inclusion. All ^{1}H chemical shifts are reported in Table 2.

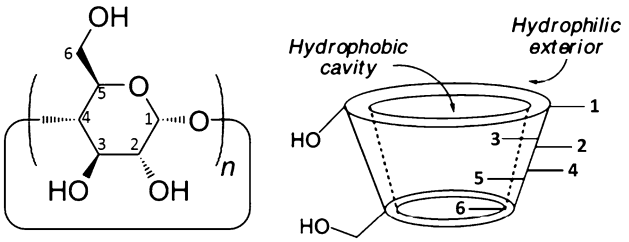

Fig. 6 Structures of the glucopyranose repeating unit (for β-CD, n = 7), and the toroidal structure of β-CD emphasizing the position of inner hydrogens 3 and 5

The ^{1}H NMR spectroscopic measurements also allow inferring about the stability of the inclusion complex and the orientation of the drug molecule. According to Greatbanks and Pickford [44], the evaluation of Δδ of the inner hydrogens of β-CD (Δδ = δ inclusion complex − δ free β-CD) can give relevant information about the inclusion, allowing conclusions about the stability. When Δδ 3 > Δδ 5, a partial inclusion of the guest inside the cavity is occurring. On the other hand, when Δδ 3 < Δδ 5, a total inclusion takes place. The values reported in Table 2 show that Δδ 3 < Δδ 5, which indicates a total inclusion of the guest in the cavity.

The presence of two aromatic rings in the Ag-NMS molecule (Fig. 1) turns possible the formation of 1:1 or 1:2 guest/host stoichiometries for the inclusion complexes. Also, since one of the rings is more substituted than the other, an inclusion preference could take place. Comparing the ^{1}H signals of the free Ag-NMS with the inclusion complex, we can see that the highest shifts occur for H6 and H3 of the higher substituted ring, and for H2′ and H6′ of the phenoxy ring. No interaction is observed with the exterior hydrogens 2 and 4 of cyclodextrin. One important information is that no shift is observed for H4′ of Ag-NMS, thus indicating no interaction of this hydrogen with β-CD, while the other protons of the same ring interact. This result suggests a total inclusion of the phenoxy ring into the cavity of β-CD.

NOESY NMR spectroscopic data

In order to further confirm the binding mode in the [(Ag-NMS)·β-CD], a 2D NOESY experiment was performed for the inclusion complex. The spectrum is presented in Fig. 9.

It is clearly observed that the inner cavity hydrogens 3 and 5 of the cyclodextrin correlate with protons of the phenoxy ring of nimesulide in the Ag-NMS complex. There is also an interaction between the hydrogen 5 of β-CD with H6 of Ag-NMS. The strongest correlation is observed for hydrogens H2′ and H6′ of Ag-NMS with the hydrogen 3 of the β-CD. No correlation is observed for H4′of Ag-NMS, thus confirming the proposition from ^{1}H

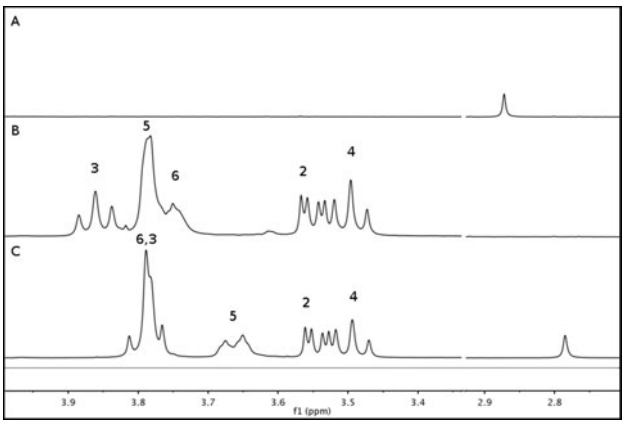

Fig. 7 ^{1}H NMR spectra of the **a** Ag-NMS, **b** β-CD and **c** *CE*-[(Ag-NMS)·β-CD] from 2.5 to 4.0 ppm

NMR of the total inclusion of the phenyl ring into the cavity with no interaction of H4′ with any proton of β-CD.

Antibacterial assays

Antibiogram assays were carried out in order to evaluate the antibacterial activities of the compounds Ag-NMS, *CE*-[(Ag-NMS)·β-CD] and *CE*-[(NMS)·β-CD] and also to further compare the observed results of *CE*-[(Ag-NMS)·β-CD] to that described for the free Ag-NMS coordination compound [37]. The antibacterial activities were confirmed by the MIC values. The results are shown in Table 3.

The Ag-NMS coordination compound presents MIC values in the range 6.25–50.0 μg mL^{-1}. The inhibition of *E. coli*, *S. aureus* and *P. aeruginosa* bacterial strain are in accordance with the previously reported activity of the complex by the disc diffusion method [37].

Although more soluble in water, the inclusion complex *CE*-[(Ag-NMS)·β-CD] did not show activity under the same bacterial strains in the same experimental conditions. Both the free Ag-NMS and the inclusion complex *CE*-[(Ag-NMS)·β-CD] were assayed from 10 mg mL^{-1} stock solutions. The Ag-NMS is the bioactive species, what means that upon inclusion, the available concentration of

Table 2 ^{1}H assignments, chemical shifts and multiplicity for Ag-NMS, β-CD and [β-CD·(NMS)]

Ag-NMS	Multiplicity	δ Ag-NMS/ppm	δ [β-CD·(Ag-NMS)]/ppm	Δδ
H5	dd	7.92	7.92	0.00
H6	d	7.59	7.73	0.14
H3	d	7.42	7.53	0.11
H3′, H5′	t	7.29	7.34	0.05
H4′	t	7.09	7.07	−0.02
H2′, H6′	d	6.94	6.82	−0.12
β-CD	**Multiplicity**	**δ β-CD/ppm**	**δ [β-CD·(Ag-NMS)]/ppm**	**Δδ**
1	d	4.98	4.97	−0.01
3	t	3.86	3.78	−0.08
6	s	3.78	3.79	0.01
5	dt	3.76	3.66	−0.10
2	dd	3.55	3.55	0.00
4	t	3.50	3.49	−0.01

Δδ is the difference (in ppm) of the chemical shifts between [β-CD·(NMS)] and Ag-NMS or between [β-CD·(Ag-NMS)] and β-CD

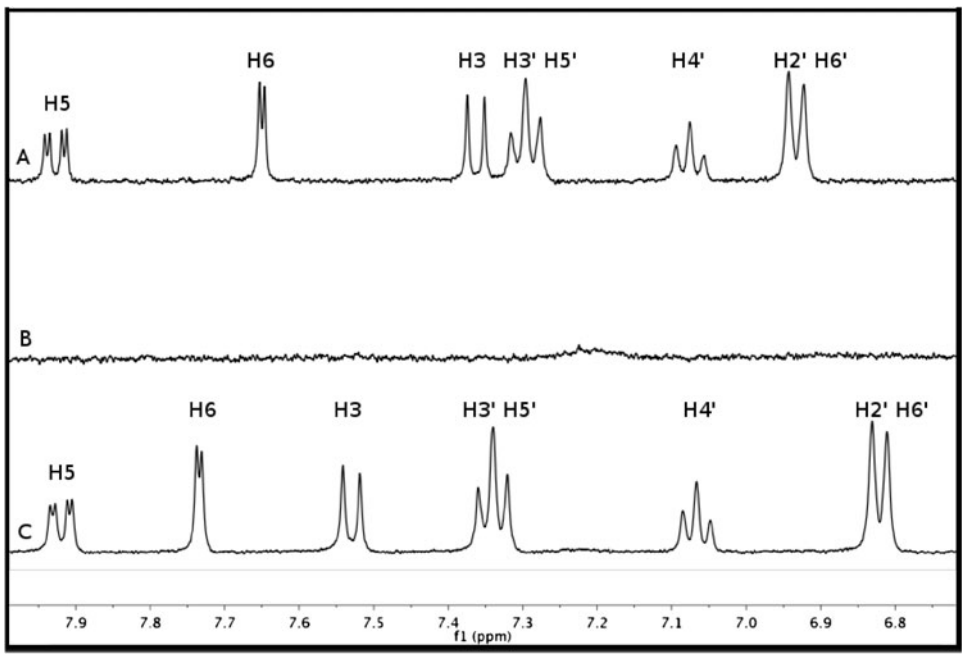

Fig. 8 ^{1}H NMR spectra of the **a** Ag-NMS, **b** β-CD and **c** *CE*-[(Ag-NMS)·β-CD] from 6.0 to 8.0 ppm

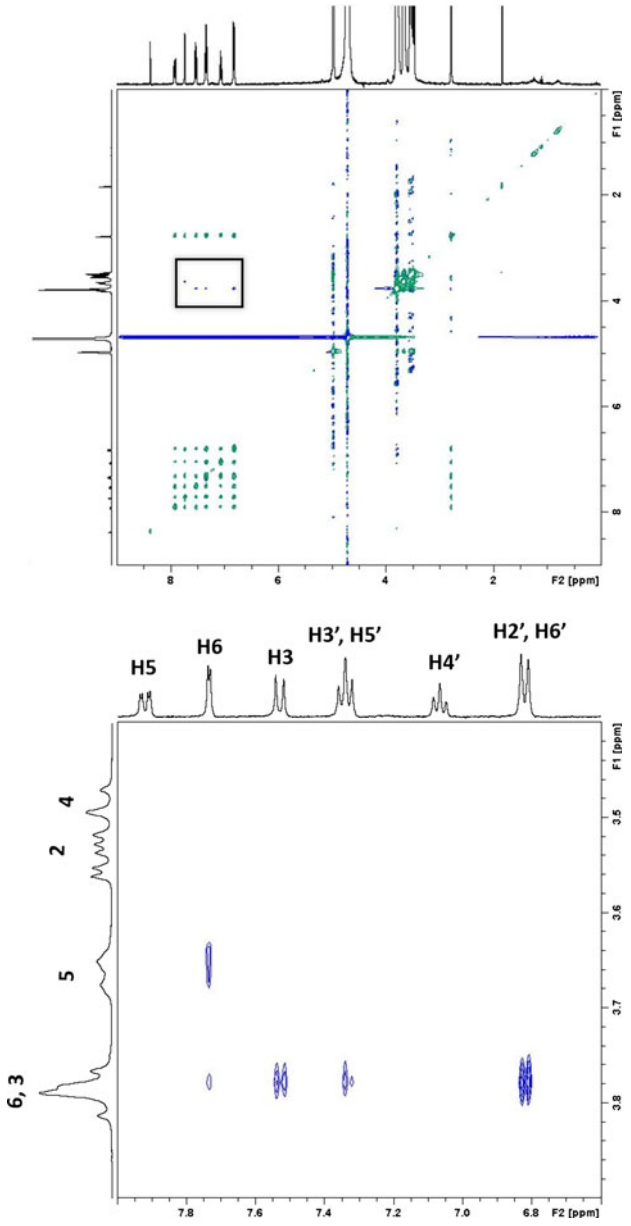

Fig. 9 2D-NOESY spectrum of *CE*-[(Ag-NMS)·β-CD] in D_2O at room temperature with a mixing time of 800 ms. *Top* full spectrum; *bottom* NOE signals that demonstrate correlation between β-CD hydrogens (3, 5 and 6) and Ag-NMS hydrogens

Ag-NMS is lower. This can justify the lack of antibacterial activity observed for the inclusion complex. Further studies may be envisaged in order to confirm if the activities of both *CE*-[(Ag-NMS)·β-CD] and Ag-NMS compounds vary linearly with the silver content. The inclusion complex *CE*-[(NMS)·β-CD] did not present activity against the considered bacterial strains, since the free nimesulide does not show antibacterial activities as previously reported [37].

Conclusions

New inclusion complexes of NMS and Ag-NMS were obtained. For the Ag-NMS inclusion complexes, the DSC data show that the material obtained by kneading (*K*-[(Ag-NMS)·β-CD]) in 1:2 molar ratio presents a sharper melting peak. Also, the DSC of both materials prepared by kneading do not present the melting of the precursors (β-CD and Ag-NMS), which is an indicative of the formation of inclusion complexes. The Ag-NMS co-evaporated system shows no melting peaks and could not be evaluated properly by DSC. The XRD data show that the *K*-[(Ag-NMS)·β-CD] 1:1 formulation presents no crystallinity, while the *K*-[(Ag-NMS)·β-CD] 1:2 formulation presents the diffraction pattern similar to β-CD. The IR data shows that nimesulide remains coordinated to Ag(I) by the nitrogen and oxygen atoms of the sulfonamide group upon inclusion.

The association constants found for NMS and Ag-NMS were of 367 ± 3 and 370 ± 2 L mol^{-1} respectively, demonstrating the stability of the inclusion complexes. The 2D NOESY clearly shows that the phenoxy ring of nimesulide in Ag-NMS interacts with the interior of the cavity of β-CD, and also shows that there is a correlation between the hydrogen 5 of β-CD with the H6 of Ag-NMS. The structural information given by the NMR data lead us to propose the structure shown in Fig. 10 for the [(Ag-NMS)·β-CD] inclusion system. Even though more soluble, the inclusion complex *CE*-[(Ag-NMS)·β-CD] did not present antibacterial activity when compared to the free Ag-NMS, which may be related to the low content of silver in the inclusion complex.

Table 3 Minimum inhibitory concentration of the compounds Ag-NMS, *CE*-[(Ag-NMS)·β-CD] and *CE*-[(NMS)·β-CD]

Sample	Minimum inhibitory concentration (μg mL^{-1})				
	Gram-negative		Gram-positive		
	P. aeruginosa ATCC 27853	*E. coli* ATCC 25922	*S. aureus* BEC 9393	*S. aureus* Rib1	*S. aureus* ATCC 25923
Ag-NMS	25.0	6.25	50.0	25.0	50.0
CE-[(Ag-NMS)·β-CD]	[a]	[a]	[a]	[a]	[a]
CE-[(NMS)·β-CD]	[a]	[a]	[a]	[a]	[a]
Chloramphenicol	50.0	12.5	–	–	–
Vancomycin	–	–	<10.0	<10.0	<10.0

For Gram-negative and Gram-positive bacteria chloramphenicol and vancomycin were used, respectively, as positive controls

[a] Did not present inhibitory activity under tested concentrations

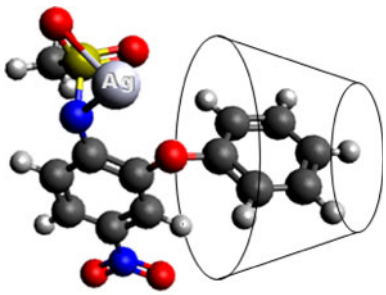

Fig. 10 Schematic representations of the phenoxy ring of Ag-NMS complex included into β-CD cavity

Acknowledgments This study was supported by grants from the Brazilian Agencies FAPESP (São Paulo State Research Foundation, Brazil—proc. 2012/08230-2), CAPES and CNPq. Professor Corbi is also grateful to Professors Celso A. Bertran and André L. B. Formiga from the Campinas State University, UNICAMP, Brazil, for technical support.

References

1. Fox, C.L.J.: Silver sulfadiazine-a new topical therapy for pseudomonas in burns. Arch. Surg. **96**, 184–188 (1968)
2. Fox, C.L., Modak, S.M.: Mechanism of silver sulfadiazine action on burn wound infections. Antimicrob. Agents Chemother. **5**, 582–588 (1974)
3. Demain, A.L., Sanchez, S.: Microbial drug discovery: 80 years of progress. J. Antibiot. **62**, 5–16 (2009)
4. Nishaminy, K.: Tigecycline: A new glycylcycline antimicrobial agent. Am. J. Health Syst Pharm **63**, 1235–1243 (2006)
5. Bergamini, F.R.G., Ferreira Jr, M.A., de Paiva, R.E.F., Gomes, A.F., Gozzo, F.C., Formiga, A.L.B., Corbi, F.C.A., Mazali, I.O., Alves, D.A., Lancellotti, M., Corbi, P.P.: A binuclear silver complex with L-buthinonine sulfoximine: Synthesis, spectroscopic characterization, DFT studies and antibacterial assays. RSC Adv. **2**, 10372–10379 (2012)
6. Pettinari, C., Marchetti, F., Lupidi, G., Quassinti, L., Bramucci, M., Petrelli, D., Vitali, L.A., da Silva, M.F.C.G., Martins, L.M.D.R.S., Smolénski, P., Pombeiro, A.J.L.: Synthesis, antimicrobial and antiproliferative activity of novel silver(I) tris(pyrazolyl) methanesulfonate and 1,3,5-triaza-7-phosphadamantane complexes. Inorg. Chem. **50**, 11173–11183 (2011)
7. Hao, H.-J., Sun, D., Li, Y.-H., Huang, R.-B., Zheng, L.-S.: Effect of different carboxylates on a series of Ag(I) coordination compounds with benzoguanamine ligand. Cryst. Growth Des. **11**, 3564–3578 (2011)
8. Jin, S., Wang, D., Shen, B., Li, Y., Yu, F., Ji, S., Su, M.J.: Synthesis and structural characterization of three saccharinate-metal complexes with exo-bidentate bis(imidazole) derivatives. J. Coord. Chem. **64**, 617–629 (2011)
9. Yaghi, O.M., Li, H.: T-shaped molecular building units in the porous structure of Ag(4,4′-bpy) NO_3. J. Am. Chem. Soc. **118**, 295–296 (1996)
10. Li, B., Zang, S.-Q., Ji, C., Du, C.-X., Hou, H.-W., Mak, T.C.W.: Syntheses, structures and properties of two unusual silver–organic coordination networks: 1D–1D tubular intertwinement and existence of an infinite winding water chain. Dalton Trans. **40**, 788–792 (2011)
11. Sengul, A., Kurt, O., Buyukgungor, O.: A 2D network silver coordination polymer with the multimodal ligand 2-pyrazyl methyl ketazine. Struct. Chem. **22**, 925–929 (2011)
12. Kasuga, N.C., Takagi, Y., Tsuruta, S.-I., Kuwana, W., Yoshikawa, R., Nomiya, K.: Synthesis, structure and antimicrobial activities Of meso silver(I) histidinate [Ag 2(D-His)(L-His)]$_N$ (Hhis = histidine) showing different self-assembly from those of chiral silver(I) histidinates. Inorg. Chim. Acta **368**, 44–48 (2011)
13. Kasuga, N.C., Yoshikawa, R., Sakai, Y., Nomiya, K.: Syntheses, structures, and antimicrobial activities of remarkably light-stable and water-soluble silver complexes with amino acid derivatives, silver(I) *N*-acetylmethioninates. Inorg. Chem. **51**, 1640–1647 (2012)
14. Maheshwari, A., Sharma, M., Sharma, D.: Investigation of the binding of roxatidine acetate hydrochloride with cyclomaltoheptaose (β-cyclodextrin) using IR And NMR spectroscopy. Carbohydr. Res. **346**, 1809–1813 (2011)
15. Szejtli, J.: Introduction and general overview of cyclodextrin chemistry. Chem. Rev. **98**, 1743–1753 (1998)
16. Szejtli, J.: Cyclodextrin technology, 1st edn. Kluwer Academic Publishers, Dordrecht (1998)
17. Wenz, G.: Cyclodextrins as building blocks for supramolecular structures and functional units. Angew. Chem. Int. Ed. Engl. **33**, 803–822 (1994)
18. Harata, K., Kawano, K.: Crystal structure of the cyclomaltohexaose (α-cyclodextrin) complex with isosorbide dinitrate. Guest-modulated channel-type structure. Carbohydr. Res. **337**, 537–547 (2002)
19. Meindersma, G.W., van Schoonhoven, T., Kuzmanovic, B., Haan, A.B.: Extraction of toluene, o-xylene from heptane and benzyl alcohol from toluene with aqueous cyclodextrins. Chem. Eng. Process. **45**, 175–183 (2006)
20. Wintgens, V., Layre, A.-M., Hourdet, D., Amiel, C.: Cyclodextrin polymer nanoassemblies: Strategies for stability improvement. Biomacromolecules **13**, 528–534 (2012)
21. McCormack, S., Russel, N.R., Cassidy, J.F.: Cyclic voltammetry of ferrocene carboxylic acid cyclodextrin inclusion complexes. Electrochim. Acta **11**, 1939–1944 (1992)
22. Ferreira, P., Gonçalves, I.S., Pillinger, M., Rocha, J., Santos, P., Teixeira-Dias, J.J.C.: Modification of β-cyclodextrin with ferrocenyl groups by ring opening of an encapsulated [1]ferrocenophane. Organometallics **19**, 1455–1457 (2000)
23. Braga, S.S., Gonçalves, I.S., Ribeiro-Claro, R., Lopes, A.D., Pillinger, M., Teixeira-Dias, J.J.C., Rocha, J., Romão, C.C.: Encapsulation of cyano(cyclopentadienyl) complexes of iron with beta-cyclodextrin. Supramol. Chem. **14**, 359–366 (2002)
24. Cunha-Silva, L., Gonçalves, I.S., Pillinger, M., Xue, W.-M., Rocha, J., Teixeira-Dias, J.J.C., Kühn, F.E.: Synthesis and characterization of the inclusion compound of a methyltrioxorhenium(VII) adduct of 4-ferrocenylpyridine with beta-cyclodextrin. J. Organomet. Chem. **656**, 281–287 (2002)
25. Fernandes, J.A., Lima, S., Braga, S.S., Pillinger, M., Ribeiro-Claro, P., Rodriguez-Borges, J.E., Lopes, A.D., Teixeira-Dias, J.J.C., Gonçalves, I.S.: Inclusion complexation of dimeric and trimeric oligo(ferrocenyldimethylsilanes) with gamma-cyclodextrin. Organometallics **24**, 5673–5677 (2005)
26. Braga, S.S., Paz, F.A.A., Pillinger, M., Seixas, J.D., Romão, C.C., Gonçalves, I.S.: Structural studies of beta-cyclodextrin and permethylated beta-cyclodextrin inclusion compounds of cyclopentadienyl metal carbonyl complexes. Eur. J. Inorg. Chem **2006**, 1662–1669 (2006)
27. Lima, S., Gonçalves, I.S., Ribeiro-Claro, P., Pillinger, M., Lopes, A.D., Ferreira, P., Teixeira-Dias, J.J.C., Rocha, J., Romão, C.C.: Interactions of cationic and neutral molybdenum complexes with beta-cyclodextrin host molecules. Organometallics **20**, 2191–2197 (2001)
28. Braga, S.S., Marques, M.P.M., Souza, J.B., Pillinger, M., Teixeira-Dias, J.J.C., Gonçalves, I.S.: Inclusion of molybdenocene dichloride (Cp2MoCl2) in 2-hydroxypropyl- and trimethyl-beta-

cyclodextrin: Structural and biological properties. J. Organomet. Chem. **690**, 2905–2912 (2005)
29. Braga, S.S., Gago, S., Seixas, J.D., Valente, A.A., Pillinger, M., Santos, T.M., Gonçalves, I.S., Romão, C.C.: Beta-cyclodextrin and permethylated beta-cyclodextrin inclusion compounds of a cyclopentadienyl molybdenum tricarbonyl complex and their use as cyclooctene epoxidation catalyst precursors. Inorg. Chim. Acta **359**, 4757–4764 (2006)
30. Braga, S.S., Ferreira, R.A.S., Gonçalves, I.S., Ribeiro-Claro, P., Pillinger, M., Rocha, J., Teixeira-Dias, J.J.C., Carlos, L.D.: Study of the inclusion compound formed between a luminescent europium (III) beta-diketonate complex and gamma-cyclodextrin. J. Incl. Phenom. Macrocycl. Chem. **44**, 261–265 (2002)
31. Morales, A., Struppe, J., Meléndez, E.: Host–guest interactions between niobocene dichloride and α-, β-, and γ-cyclodextrins: Preparation and characterization. J. Incl. Phenom. Macrocycl. Chem. **60**, 263–270 (2008)
32. Turel, I., Demšar, A., Košmrlj, T.: The Interactions of titanocene dihalides with α-, β- and γ-cyclodextrin host molecules. J. Incl. Phenom. Macrocycl. Chem. **35**, 595–604 (1999)
33. Lippold, I., Vlay, K., Görls, H., Plass, W.: Cyclodextrin inclusion compounds of vanadium complexes: Structural characterization and catalytic sulfoxidation. J. Inorg. Biochem. **103**, 480–486 (2009)
34. Marques, J., Anjo, L., Marques, M.P.M., Santos, T.M., Paz, F.A.A., Braga, S.S.: Structural studies on supramolecular adducts of cyclodextrins with the complex [Ru([9]aneS3)(bpy)Cl]Cl. J. Organomet. Chem. **693**, 3021–3028 (2008)
35. Legrand, F.-X., Ménand, M., Sollogoub, M., Tilloy, S., Monflier, E.: An N-heterocyclic carbene ligand based on a b-cyclodextrin–imidazolium salt: Synthesis, characterization of organometallic complexes and Suzuki coupling. New J. Chem. **35**, 2061–2065 (2011)
36. Whittle, B.J.R.: Gastrointestinal effects of nonsteroidal anti-inflammatory drugs. Fundam. Clin. Pharmacol. **17**, 301–313 (2003)
37. de Paiva, R.E.F., Abbehausen, C., Gomes, A.F., Gozzo, F.C., Lustri, W.R., Formiga, A.L.B., Corbi, P.P.: Synthesis, spectroscopic characterization, DFT studies and antibacterial assays of a novel silver(I) complex with the anti-inflammatory nimesulide. Polyhedron **36**, 112–119 (2012)
38. Nalluri, B.N., Chowdary, K.P.R., Murthy, K.V.R., Hayman, A.R., Becket, G.: Physicochemical characterization and dissolution properties of nimesulide-cyclodextrin binary systems. AAPS PharmSciTech. **4**, 6–17 (2003)
39. Clinical and Laboratory Standards Institute (CLSI), Performance standards for antimicrobial susceptibility testing, 17th Informational Supplement, Wayne, PA, USA (2007)
40. Sanphui, P., Sarma, B., Nangia, A.: Phase transformation in conformational polymorphs of nimesulide. J. Pharm. Sci. **100**, 2287–2299 (2011)
41. Scatchard, G.: The attractions of proteins for small molecules and ions. Ann. N. Y. Acad. Sci. **51**, 660–662 (1949)
42. Chen, M., Diao, G., Zhang, E.: Study of inclusion complex of b-cyclodextrin and nitrobenzene. Chemosphere **63**, 522–529 (2006)
43. Buvari, A., Barcza, L.: Complex formation of phenol, aniline, and their nitro derivatives with β-cyclodextrin. J. Chem. Soc. Perkin Trans. **II**, 543–545 (1988)
44. Greatbanks, D., Pickford, R.: Cyclodextrins as chiral complexing agents in water, and their application to optical purity measurements. Magn. Reson. Chem. **25**, 208–215 (1987)